

## IX-E Development of New Nanomaterials as Components in Advanced Molecular Systems

Nanometer-sized materials exhibit unique electronic behavior. In the quest of advanced redox catalysis, we are currently interested in combining nanometer-sized materials into molecular redox systems. As a basic architecture, composites of organic molecules and gold nanoparticles were synthesized and molecular dynamic simulations were carried out to predict the solution structures.

### IX-E-1 Automated Design of Protecting Molecules for Metal Nanoparticles by Combinatorial Molecular Simulations

NAGATA, Toshi

[*J. Organomet. Chem.* in press]

New tripod oligo(dibenzyl sulfide) molecules were designed by computer modeling calculations so that they would form 1:1 complexes with an Au<sub>147</sub> nanoparticle. Twelve aromatic molecules containing two methylthiomethyl groups were used as construction units ("residues"). Combinations of the residues ("sequences") were examined by molecular dynamic simulations, and those sequences giving the largest interaction energies with the gold nanoparticle were sought through either full search or genetic algorithm. Best-fit sequences were found for  $N = 5$  and 6 ( $N$  is the number of "residues" in one leg of the tripod molecule).

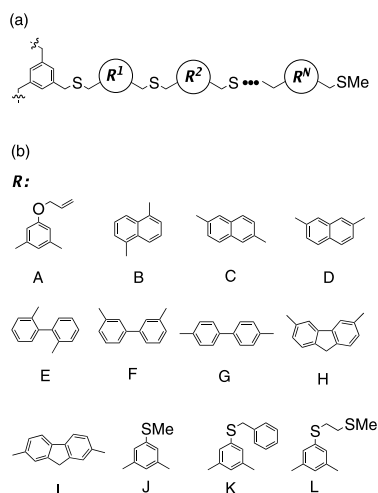


**Figure 1.** (a) The base structure of the protecting molecule. (b) The "residues" used in this study.

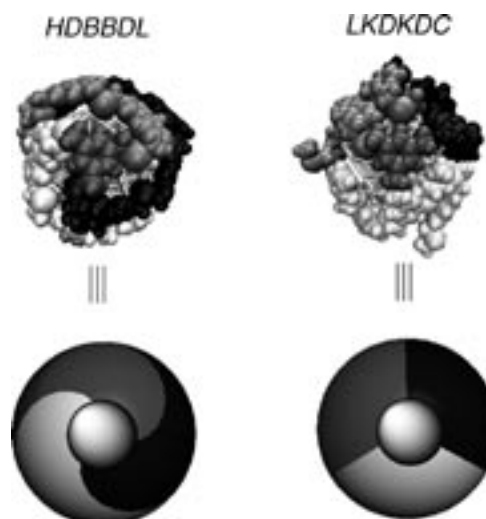


**Figure 2.** The surface covering schemes for the two lowest energy structures for  $N = 6$ . The atoms in the three "legs" are drawn in white, gray, and black, respectively.

## IX-F Designing Artificial Photosynthesis at Molecular Dimensions

Photosynthesis is one of the finest piece of molecular machinery that Nature has ever created. Its ultrafast electron transfer and following well-organized sequence of chemical transformation have been, and will continue to be, challenging goals for molecular scientists. Our ultimate goal is to design artificial molecular systems that effect multiple chemical reactions triggered by light on the basis of molecular rationale.

### IX-F-1 Elucidation of Solution Structures of Dendrimer-Linked Porphyrins

KIKUZAWA, Yoshihiro; NAGATA, Toshi; TAHARA, Tahei<sup>1</sup>; ISHII, Kunihiko<sup>1</sup>  
(<sup>1</sup>RIKEN)

[Chem. Asian J. in press]

In order to estimate the average structures of our ferrocene-dendrimer-porphyrins (Figure 1), we carried molecular-dynamic (MD) simulations of these molecules in  $\text{CHCl}_3$  solutions. Figure 2 shows the spatial distribution of the iron atoms of all the ferrocenyl groups, in relative to the porphyrin ring at the core. Figure 3 shows the radial distribution functions of the iron atoms in the first, second, and third layers from the center of the porphyrin ring. These figures clearly show that only the ferrocenyl groups in the second layer have significant probability to approach the porphyrin ring closer than 10 Å. This observation is consistent with the results of <sup>1</sup>H NMR and fluorescence quenching, namely the second layer had a larger interaction with the porphyrin ring than the first and third layers.

It is also interesting to note that such layered distribution was more distinct in  $\text{G3}(\text{Fc})_{14}\text{-ZnP}$  than in  $\text{G2}(\text{Fc})_6\text{-ZnP}$ , the generation 2 compound with the similar architecture. The spatial distribution and radial distribution functions of the iron atoms in  $\text{G2}(\text{Fc})_6\text{-ZnP}$  also showed similar trends as  $\text{G3}(\text{Fc})_{14}\text{-ZnP}$ , although the distribution of the first layer Fe atoms was somewhat broader in  $\text{G2}(\text{Fc})_6\text{-ZnP}$  than in  $\text{G3}(\text{Fc})_{14}\text{-ZnP}$ . These results suggest that, even in the case of these “spatially relaxed” dendritic frameworks, the presence of the higher-generation branches restricts the movements of the inner layer.

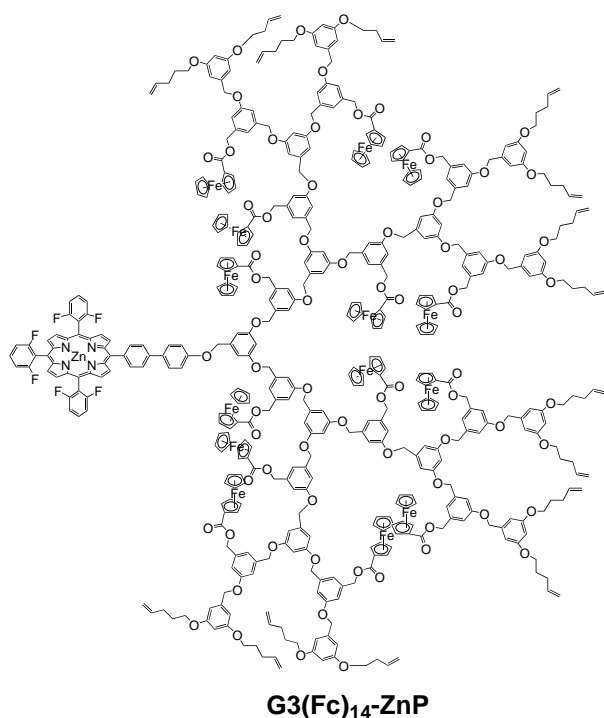


**Figure 1.** The structure of the ferrocene-dendrimer-linked porphyrin (generation 3).

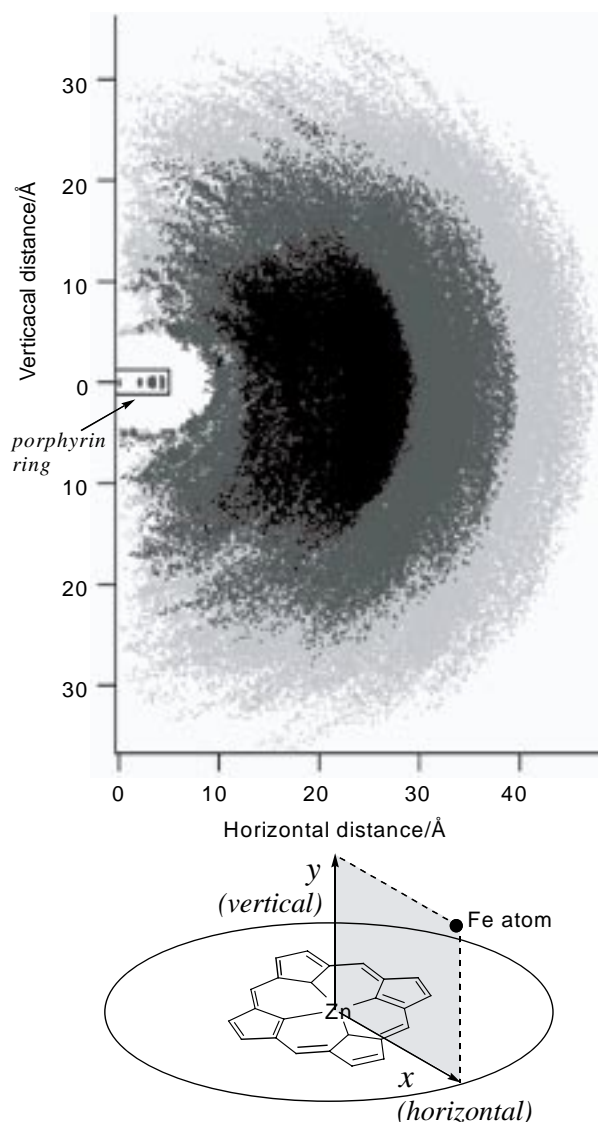


**Figure 2.** The calculated distribution of the iron atoms of the ferrocenyl groups in  $\text{G3}(\text{Fc})_{14}\text{-ZnP}$ . The first, second, and third layer are represented by dark gray, medium gray, and light gray respectively.

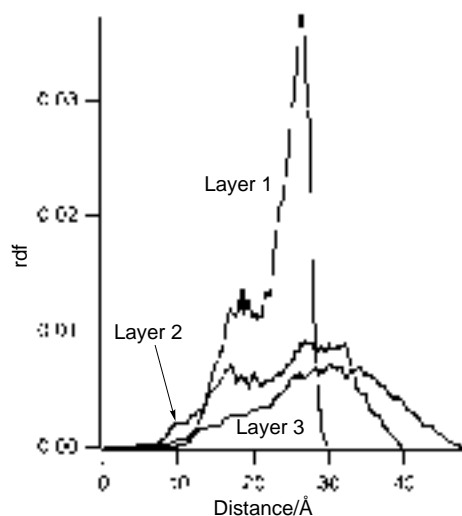


**Figure 3.** Radial distribution function (per single atom) of the iron atoms in each layer in  $\text{G3}(\text{Fc})_{14}\text{-ZnP}$ .

### IX-F-2 Reconstitution of the Water-Oxidizing Complex in Manganese-Depleted Photosystem II Preparations Using Binuclear Mn(II) and Mn(IV) Complexes

NAGATA, Toshi; NAGASAWA, Takayuki;  
ZHARMUKHAMEDOV, Sergei K.<sup>1</sup>;  
ALLAKHVERDIEV, Suleyman I.<sup>2</sup>

(<sup>1</sup>Inst. Basic Biological Problems, Russian Acad. Sci.;  
<sup>2</sup>IMS and Inst. Basic Biological Problems, Russian Acad. Sci.)

Reconstitution of the Mn-depleted Photosystem II (PSII) particles with synthetic binuclear Mn complexes (two Mn(II)<sub>2</sub> complexes and one Mn(IV)<sub>2</sub> complex) was examined. The reconstituted PSII particles showed lower restored activities than our previous studies in photo-induced electron transfer and oxygen evolution. These results were ascribed to the "robustness" of the Mn complexes used in this study. The ESI-MS spectra of the Mn(II)<sub>2</sub> complexes showed that the macrocyclic ligand remained intact even after release of the Mn(II) ions, so it was proposed that the macrocyclic ligand remained in the vicinity of the PSII proteins and caused distortion of the protein structures. On the other hand, the lower activity of the Mn(IV)<sub>2</sub> complex was ascribed to the robustness of the bis- $\mu$ -oxo structure which caused transfer of the Mn ions to the PSII protein less efficient than the previously examined Mn complexes with mono-nuclear or mono- $\mu$ -oxo binuclear structures. These results implies that subtle balance between the stability and lability of the complexes are important in successful reconstitution of PSII.

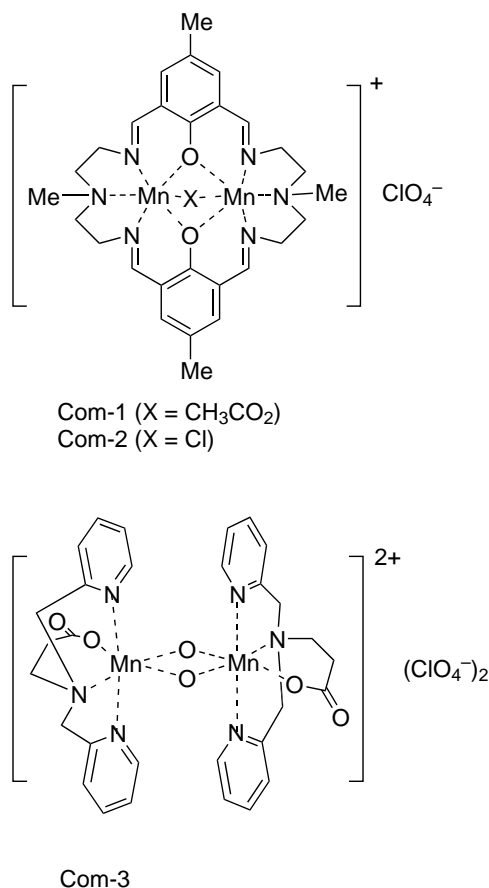


**Figure 1.** The structures of the synthetic dimanganese complexes.

## IX-G Development of New Metal Complexes as Redox Catalysts

Redox catalysis is an important field of chemistry which translates a flow of electron into chemical transformation. It is also one of the requisites for artificial photosynthesis. This project of ours aims at developing new metal complexes that perform redox catalysis at low overpotential. Currently we are focusing our attention to the development of a series of cobalt phosphine complexes as possible catalysts for electrochemical reductions.

### IX-G-1 Syntheses and Structures of Co(I) Complexes Having Cyclopentadienyl Auxiliaries and C-P Bond Cleavage of the Coordinated Phosphine

NAGASAWA, Takayuki; NAGATA, Toshi

The strong basicity of low-valent cobalt complexes are attractive in electrocatalytic organometallic chemistry. Here we report the syntheses and molecular structures of Co(I) complexes with cyclopentadienyl derivatives and an unexpected cleavage of a C-P bond in triphenylphosphine by Co(I) under mild conditions.

Reactions of ClCo(PPh<sub>3</sub>)<sub>3</sub> with sodium salts of cyclopentadienyl derivatives NaCp<sup>R</sup> (R = H, COOMe, CH<sub>2</sub>CH<sub>2</sub>SMe) gave five-coordinate Co(I) complexes

Cp<sup>R</sup>Co(PPh<sub>3</sub>)<sub>2</sub> (R = H, **2**; COOMe, **3**; CH<sub>2</sub>CH<sub>2</sub>SMe, **4**) in 60–80% yields as crystals. The structures of **2–4** were determined by X-ray crystallography (Figure 1).

On the other hand, the reaction of LiCp\* (Cp\* = C<sub>5</sub>Me<sub>5</sub>) with ClCo(PPh<sub>3</sub>)<sub>3</sub> resulted in a formation of a diamagnetic dimer complex [Cp\*Co(μ-Ph)(μ-PPh<sub>2</sub>)CoCp\*], **5**, which has bridging phenyl and diphenylphosphide groups. This compound was isolated from hexane solution as black crystals in 64% yield. The structure was confirmed by X-ray crystallography (Figure 2). We propose that the bridging phenyl and phosphide ligands were generated by a C-P bond cleavage caused by the action of the strongly nucleophilic Cp\*Co fragment.

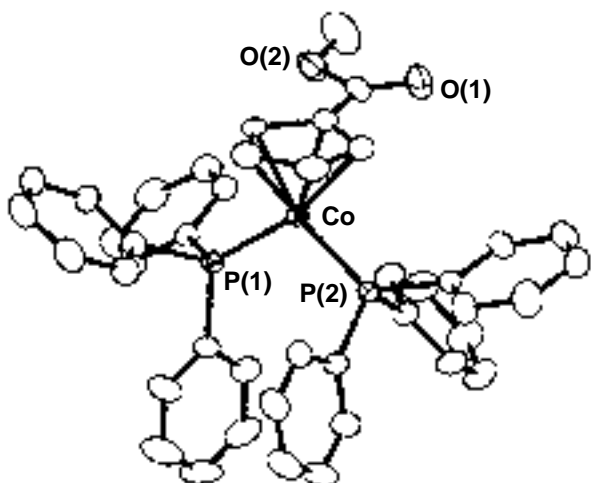


Figure 1. The ORTEP drawing of 3.

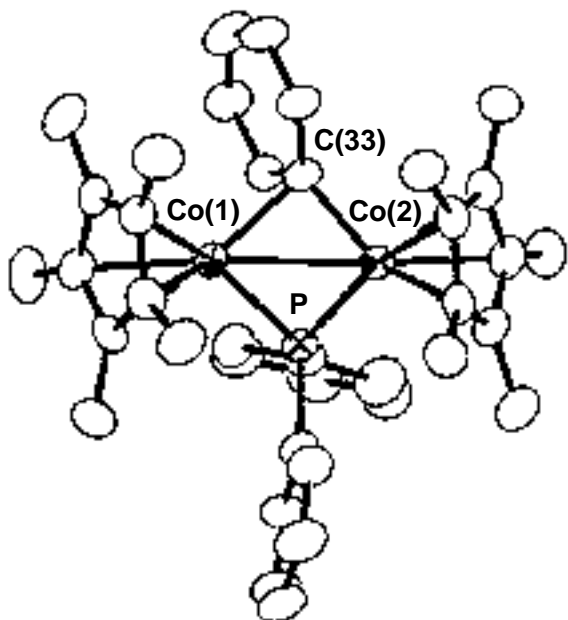


Figure 2. The ORTEP drawing of 5.